Microscopic theory of the residual surface resistivity of Rashba electrons

Juba Bouaziz,[*] Samir Lounis,[†] and Stefan Blügel

Peter Grünberg Institut and Institute for Advanced Simulation, Forschungszentrum Jülich and JARA, 52425 Jülich, Germany

Hiroshi Ishida

College of Humanities and Sciences, Nihon University, Sakura-josui, Tokyo 156-8550, Japan
and Center for Materials Research by Information Integration, National Institute for Materials Science, Tsukuba, Ibaraki 305-0047, Japan

A microscopic expression of the residual electrical resistivity tensor is derived in linear response theory for Rashba electrons scattering at a magnetic impurity with cylindrical or noncylindrical potential. The behavior of the longitudinal and transversal residual resistivity is obtained analytically and computed for an Fe impurity at the Au(111) surface. We studied the evolution of the resistivity tensor elements as a function of the Rashba spin-orbit strength and the magnetization direction of the impurity. We found that the absolute values of longitudinal resistivity reduce with increasing spin-orbit strength of the substrate and that the scattering of the conduction electrons at magnetic impurities with magnetic moments pointing in directions not perpendicular to the surface plane produce a planar Hall effect and an anisotropic magnetoresistance even if the impurity carries no spin-orbit interaction. Functional forms are provided describing the anisotropy of the planar Hall effect and the anisotropic magnetoresistance with respect to the direction of the impurity moment. In the limit of no spin-orbit interaction and a nonmagnetic impurity of cylindrical symmetry, the expression of the residual resistivity of a two-dimensional electron gas has the same simplicity and form as for the three-dimensional electron gas [J. Friedel, J. Nuovo. Cim. **7**, 287 (1958)] and can also be expressed in terms of scattering phase shifts.

I. INTRODUCTION

The electron transport in metals and semiconductors is an important field of research since it crucially influences the efficiency, power consumption, size, and lifetime of electronic components. The use of the spin degree of freedom in addition to the charge is expected to boost microelectronics by adding new functionalities to existing devices. An important building block relating charge to spin currents is the spin-orbit (SO) interaction that appears also in terms of the Rashba effect [1,2] in surface and interface states of heavy metals or in semiconductors in contact with those. The Rashba effect arises from the SO coupling in an environment with a lack of space-inversion symmetry such as interfaces and surfaces where Bloch-momentum-dependent spin splittings, known as the Rashba spin splitting, are observed in the band structure. The Rashba spin splitting at surfaces was first observed for the two-dimensional (2D) Shockley surface state of the Au(111) surface [3–6]. It was investigated for a number of clean [5,7,8] and alloyed surfaces [9,10], adsorbed surface layers [11,12], and surface states of semiconductors in contact with heavy metals [13]. For some of those systems, large spin splittings had been observed. By this, the Rashba splitting makes possible the efficient application of the Edelstein effect [14] mediated creation of large lateral spin polarization.

The scattering of Rashba electrons at impurities is a source of magnetotransport properties. In particular, we expect contributions to the planar Hall effect (PHE), the anomalous Hall effect (AHE), as well as the anisotropic magnetoresistance (AMR). Both the PHE and AHE are observed as a voltage transverse to the applied current [15,16], in contrast to the AMR, which is measured in the longitudinal geometry. Consequently, PHE and AHE are characterized by the transverse resistivity ρ_{xy}, while the AMR is characterized by the longitudinal one, ρ_{xx}. For PHE, the in-plane component of the magnetization $M_\parallel$ with respect to the interface plane and, for AHE, the out-of-plane component M_z matter. Although the AMR has been known since 1856 [17], the PHE was not discovered until more than a century later [18]. Only recently it was established that the PHE can originate from the AMR without contributions from the AHE [19].

Since the early 1990s, with the advent of low-temperature scanning tunneling microscopy (STM), the investigation of the scattering of surface states on impurities has proved very fruitful for studying the quantum behavior of matter. Crommie *et al.* [20] reported the direct observation of standing-wave patterns due to the scattering of the 2D electron gas off a single Fe impurity on the Au(111) surface. Recently, Lounis *et al.* [21] refined this picture by including the Rashba effect in the description of the 2D electron gas provided by the Shockley surface state of the Au(111) surface and found a magnetic-adatom-induced Skyrmion-like spin texture in the standing-wave pattern.

In this paper, we study the effect of the SO interaction on the residual resistivity of a 2D surface or interface Rashba states induced by a single nonmagnetic or magnetic impurity and their contribution to the various magnetotransport properties. The impurity may not necessarily be a single atom. It can be any defect whose potential perturbation is localized. For example, it can be an adsorbed molecule made out of several atoms. An objective of this paper is to formulate a residual resistive tensor with longitudinal and transverse resistivity contributions as an extension of a recently derived microscopic linear response expression of the surface resistivity for a

[*]j.bouaziz@fz-juelich.de
[†]s.lounis@fz-juelich.de

semi-infinite jellium model [22,23] to the 2D Rashba electron gas. The impurity in our model is described by a scattering matrix and we consider, in general, that the potential perturbation induced by the impurity does not need to fulfill any symmetry such as cylindrical symmetry with respect to the impurity position or a magnetic moment perpendicular to the surface. Moreover, the SO interaction can be incorporated at the level of the impurity besides the surrounding electron gas (see Ref. [24]). In that case, the SO coupling contribution to the scattering matrix can be added. For our application related to a single magnetic atom adsorbed on Au(111), we will, however, neglect this SO term when evaluating the residual resistivity tensor. While our focus is on the Rashba electron gas, we note that recently an interesting work was performed on the impact of impurities on the transport properties of 3D topological insulator surfaces [25].

We found that in the absence of SO interaction and of the magnetism at the impurity, the diagonal contributions of the resistivity tensor induced by a single adatom can be expressed in terms of scattering phase shifts, just like the well-known expression by Friedel [26],

$$\rho = A_{\mathrm{F}} \sum_{\ell \geqslant 0} (\ell + 1) \sin^2[\delta_{\ell+1}(\varepsilon_{\mathrm{F}}) - \delta_\ell(\varepsilon_{\mathrm{F}})], \qquad (1)$$

where the residual resistivity ρ, at $T = 0$ K, induced by a nonmagnetic impurity with a spherical potential in a 3D degenerate free-electron gas is related to the momentum-transfer cross section of electrons at the Fermi surface given by a sum over the orbital momentum quantum numbers ℓ. Here, A_{F} is a constant prefactor proportional to the inverse of the wave vector k_{F} at the Fermi energy ε_{F} of the host conduction electrons described by the free 3D electron gas. $\delta_l(\varepsilon_{\mathrm{F}})$ is the phase shift between the scattered wave function at the impurity and the unscattered host wave function.

As an application, we have considered an Fe impurity on the Au(111) surface, both nonmagnetic and magnetic, with perpendicular and arbitrary direction of the impurity moment with respect to the surface plane. If the impurity moment has a component parallel to the surface plane, the scattering matrix as well as the transverse components of the resistivity tensor are nonzero, even when the impurity potential has cylindrical symmetry and a PHE is found. We follow the longitudinal resistivity and the AMR as a function of the spin-orbit strength and the transverse resistivity and the PHE as a function of the orientation of the magnetic impurity moment with respect to the surface plane. The AHE is absent since we consider a non-spin-polarized 2D Rashba electron gas [15] and is not further considered in this paper. Also, we provide a phenomenological functional form for the different components of the residual resistivity as a function of the orientation of the magnetic moment.

The paper is organized as follows: In Sec. II, we briefly introduce the Rashba model, basically to define all quantities. Then, the ingoing and outgoing scattering states of the Rashba Hamiltonian are introduced. We express the resistivity tensor components in terms of scattering coefficients, which we relate to the scattering matrix via the Lippmann-Schwinger equation. We introduce expressions for cylindrical and noncylindrical impurity potentials of magnetic impurity moments normal to

the surface and arbitrary orientation of the magnetic impurity moment. The result of the resistivity tensor, i.e., the application of the derived expression for an Fe impurity on Au(111), is reported and discussed in Sec. III. A summary is provided in Sec. IV.

II. THEORY

A. Rashba model

The SO interaction leads, in a structure-asymmetric environment such as a surface or interface, to a spin splitting of the otherwise twofold degenerate eigenstates of a two-dimensional electron gas. The model of Bychkov and Rashba [1,2] describes this splitting by adding to the kinetic energy of the free electrons the so-called Rashba Hamiltonian,

$$\mathbf{H} = \frac{p_x^2 + p_y^2}{2m^*} \otimes \mathbb{1}_2 - \frac{\alpha_{\mathrm{so}}}{\hbar}(\boldsymbol{\sigma}_x p_y - \boldsymbol{\sigma}_y p_x), \qquad (2)$$

where p_γ, $\gamma \in \{x, y\}$, are the components of the momentum operator $\vec{p}$ in a Cartesian coordinate system with x, y coordinates in the surface plane whose surface normal points along $\hat{e}_z$. m^* is the effective mass of the electron. $\boldsymbol{\sigma}_\gamma$ are the Pauli matrices and $\mathbb{1}_2$ is the unit matrix in spin space with a global spin frame of reference where the spin z direction is aligned parallel to $\hat{e}_z$. α_{so} is the Rashba parameter, a measure of the strength of the SO interaction and the parameter that controls the degree of Rashba spin splitting.

The eigenstates corresponding to this Hamiltonian are written as a product of a plane wave in space and a two-component spinor,

$$\psi_{\vec{k},\pm}(\vec{r}) = \frac{1}{\sqrt{2}} e^{i\vec{k}\cdot\vec{r}} \begin{pmatrix} 1 \\ \pm i e^{i\phi_{\vec{k}}} \end{pmatrix} \text{ with } \phi_{\vec{k}} = \arctan\left(\frac{k_y}{k_x}\right), \quad (3)$$

i.e., they can be considered as a superposition of spin-up and -down states when measured with respect to the surface normal. The orientation of the local spin-quantization axis, given by the expectation value $\hat{n}_\pm(\vec{k}) = \langle \psi_{\pm\vec{k}} | \vec{\boldsymbol{\sigma}} | \psi_{\pm\vec{k}} \rangle = \pm(-\sin\phi_{\vec{k}}, \cos\phi_{\vec{k}}, 0) = \pm\hat{e}_\phi$, lies in the surface plane and is perpendicular to the wave vector, $\vec{k} = k(\cos\phi_{\vec{k}}, \sin\phi_{\vec{k}}, 0) = k\,\hat{e}_k$. We find that the quantization axis is independent of the magnitude k and depends only on the direction $\hat{e}_k$ of the wave vector $\vec{k}$. With respect to this quantization axis that is parallel to $\hat{e}_\phi$ in a cylindrical coordinate system, ψ_α are spin pure eigenstates and we can associate ψ_α for $\alpha = +(-)$ as the spin-up (-down) state.

The energy dispersion is characterized by the k-linear splitting of the free-electron parabolic band dispersion as denoted:

$$\varepsilon_\pm(k) = \frac{\hbar^2 k^2}{2m^*} \pm \alpha_{\mathrm{so}} k = \frac{\hbar^2}{2m^*}\big[(k \pm k_{\mathrm{so}})^2 - k_{\mathrm{so}}^2\big]. \quad (4)$$

Due to the presence of the z-inversion broken symmetry and the SO interaction, the origins of the spin-up and -down parabola are shifted by the Rashba or the spin-orbit wave vector, respectively, $k_{\mathrm{so}} = m^*\alpha_{\mathrm{so}}/\hbar^2$ and the dispersion relation describes two bands.

B. Scattering states

In order to describe the scattering problem of the Rashba electrons at a single impurity, it is convenient to exploit the cylindrical symmetry of the Rashba electron gas, to introduce the cylindrical coordinates (r, ϕ) with radius r and azimuth ϕ between the vector $\vec{r}$ and the x axis, and to place the impurity at the origin of the coordinate system. For this purpose, it is more convenient to express the eigenfunctions of the Rashba Hamiltonian (2) in terms of the cylindrical Bessel functions rather than plane waves as

$$\psi_{\varepsilon m\pm}(\vec{r}) = \frac{e^{-\frac{2m+1}{4}\pi i}}{\sqrt{2}} \begin{pmatrix} J_m(k_\pm r)e^{im\phi} \\ \mp J_{m+1}(k_\pm r)e^{i(m+1)\phi} \end{pmatrix}, \qquad (5)$$

where the state is labeled by the energy ε, band index $\alpha = \pm$, and the orbital angular quantum number m, $m \in \mathbb{Z}$, rather than the wave vector $\vec{k}$ or $(k, \phi_{\vec{k}})$. The wave number for band α is defined by

$$\begin{cases} k_\pm = k_{\mathrm{M}} \mp k_{\mathrm{so}}, \\ \text{with } k_{\mathrm{M}} = \left[\frac{2m^*\varepsilon}{\hbar^2} + k_{\mathrm{so}}^2 \right]^{1/2}, \end{cases}$$

so that $k_+ - k_- = -2k_{\mathrm{so}}$ holds irrespective of the value of $\varepsilon (> 0)$. We note that $\psi_{\varepsilon m\alpha}(\vec{r})$ is an eigenvector for the z component of the total angular momentum operator $\mathbf{j}_z = \mathbf{l}_z + \frac{\hbar}{2}\boldsymbol{\sigma}_z$ with an eigenvalue $j_z = \hbar(m + \frac{1}{2})$ and $\mathbf{l}_z$ is the orbital angular momentum operator. $\psi_{\varepsilon m\alpha}(\vec{r})$ can be decomposed into an incident and an outgoing wave: $\psi_{\varepsilon m\alpha}(\vec{r}) = \psi_{\varepsilon m\alpha}^{\mathrm{in}}(\vec{r}) + e^{-(m+\frac{1}{2})\pi i}\psi_{\varepsilon m\alpha}^{\mathrm{out}}(\vec{r})$. For each band component, the incoming and outgoing wave functions are, respectively, cylindrical Hankel functions of the second kind (see Ref. [27] for a similar derivation),

$$\psi_{\varepsilon m\pm}^{\mathrm{in}}(\vec{r}) = \frac{e^{-\frac{2m+1}{4}\pi i}}{2\sqrt{2}} \begin{pmatrix} H_m^{(2)}(k_\pm r)e^{im\phi} \\ \mp H_{m+1}^{(2)}(k_\pm r)e^{i(m+1)\phi} \end{pmatrix}, \qquad (6)$$

and the first kind,

$$\psi_{\varepsilon m\pm}^{\mathrm{out}}(\vec{r}) = \frac{e^{\frac{2m+1}{4}\pi i}}{2\sqrt{2}} \begin{pmatrix} H_m^{(1)}(k_\pm r)e^{im\phi} \\ \mp H_{m+1}^{(1)}(k_\pm r)e^{i(m+1)\phi} \end{pmatrix}. \qquad (7)$$

Their phase factors are chosen such that at large distances $(r \to \infty)$, we can express them as

$$\psi_{\varepsilon m\pm}^{\mathrm{in}}(\vec{r}) = \frac{1}{\sqrt{4\pi k_\pm r}} e^{-ik_\pm r} e^{im\phi} \begin{pmatrix} 1 \\ \mp i e^{i\phi} \end{pmatrix}, \qquad (8)$$

$$\psi_{\varepsilon m\pm}^{\mathrm{out}}(\vec{r}) = \frac{1}{\sqrt{4\pi k_\pm r}} e^{ik_\pm r} e^{im\phi} \begin{pmatrix} 1 \\ \pm i e^{i\phi} \end{pmatrix}, \qquad (9)$$

with $\psi_{\varepsilon m\pm}^{\mathrm{in}}$ and $\psi_{\varepsilon m\pm}^{\mathrm{out}}$ describing 2D cylindrical waves incoming toward and outgoing from the origin of the coordinate system, respectively. They are related by

$$\hat{T}\psi_{\varepsilon m\pm}^{\mathrm{in}}(\vec{r}) = \mp i\, \psi_{\varepsilon, -(m+1), \pm}^{\mathrm{out}}(\vec{r}),$$

where $\hat{T}$ denotes the time-reversal operator.

Now, we introduce a localized impurity for convenience placed at the origin of the cylindrical coordinate system of the 2D electron gas. We describe the elastic scattering of the wave function $\psi_{\varepsilon m\pm}$ from the impurity with the Lippmann-Schwinger equation involving real- and spin-space

coordinates:

$$\varphi_{\varepsilon m\alpha}(\vec{r}) = \psi_{\varepsilon m\alpha}(\vec{r}) + \int d\vec{r}' d\vec{r}'' \mathbf{G}_0(\vec{r}, \vec{r}', \varepsilon) \mathbf{t}(\vec{r}', \vec{r}'') \psi_{\varepsilon m\alpha}(\vec{r}''), \tag{10}$$

where $\mathbf{G}_0(\vec{r}, \vec{r}', \varepsilon)$ is the Green function of the Rashba electron gas and $\mathbf{t}(\vec{r}, \vec{r}')$ is the transition matrix (t matrix), related to the impurity potential $\mathbf{v}(\vec{r})$ via the Dyson equation: $\mathbf{t}(\vec{r}, \vec{r}') = \mathbf{v}(\vec{r})\, \delta(\vec{r} - \vec{r}') + \int d\vec{r}''\, \mathbf{v}(\vec{r})\, \mathbf{G}_0(\vec{r}, \vec{r}'', \varepsilon)\, \mathbf{t}(\vec{r}'', \vec{r}')$. In the asymptotic region where the impurity potential $\mathbf{v}(\vec{r})$ vanishes, Eq. (10) can be written in a simpler form by using scattering coefficients $C(m\alpha, m'\alpha')$. Then, the wave function of an incident electron with quantum state (ε, m, α) scattering elastically from a noncylindrical impurity potential placed at the origin is expressed as

$$\varphi_{\varepsilon m\alpha}(\vec{r}) = \psi_{\varepsilon m\alpha}^{\mathrm{in}}(\vec{r}) + \sum_{m', \alpha'} \sqrt{\frac{k_{\alpha'}}{k_\alpha}}\, C(m\alpha, m'\alpha') \psi_{\varepsilon m'\alpha'}^{\mathrm{out}}(\vec{r}), \tag{11}$$

where the factor $\sqrt{k_{\alpha'}/k_\alpha}$ accounts for the fact that the incoming and outgoing waves, $\psi_{\varepsilon m\alpha}^{\mathrm{in}}$ and $\psi_{\varepsilon m\alpha}^{\mathrm{out}}$, carry electron current k_{M}/k_α rather than unity due to the relativistic correction of the velocity operator, which will be discussed below. Here, the scattering coefficients fulfill the unitary condition,

$$\sum_{m_1\alpha_1} C(m\alpha, m_1\alpha_1)\, C^*(m'\alpha', m_1\alpha_1) = \delta_{mm'}\delta_{\alpha\alpha'}. \tag{12}$$

Specifically, the diagonal elements of the above equation with $m = m'$ and $\alpha = \alpha'$,

$$\sum_{m_1\alpha_1} |C(m\alpha, m_1\alpha_1)|^2 = 1, \tag{13}$$

ensure a current conservation.

For $\alpha \neq \alpha'$, the coefficients give weight to the interband transition during the scattering. For $m \neq m'$, the direction of $\vec{k}$ and thus the total angular momentum component of the Rashba electrons changes during the scattering process, and the scattering coefficients refer to the amplitude of the intraband scattering. When $\mathbf{v}(\vec{r})$ has a cylindrical symmetry, i.e., $\mathbf{v}(\vec{r}) = \mathbf{v}(r)$, the orbital quantum number m is conserved and $C(m\alpha, m'\alpha')$ simplifies to $C(m\alpha, m'\alpha')\delta_{m,m'}$. The scattered wave function will be a linear combination of the spin-split eigenstates denoted by the $+$ and $-$ bands. This mixing is due to the spin-flip interband transitions whose origin is the off-diagonal part of the Rashba Green $\mathbf{G}_0$ function coming from the spin-orbit interaction.

C. Connection to the scattering matrix

We present the relation between the scattering coefficients $C(m\alpha, m\alpha')$ and the t matrix $\mathbf{t}(\vec{r}, \vec{r}')$ elements in the orbital momentum representation. For this purpose, it is convenient to express the Rashba Green function in terms of solutions of the Rashba Hamiltonian (2) in the cylindrical coordinate system presented in Sec. II B. In order to derive the Green function, we fix $\vec{r}'$ and consider $\mathbf{G}_0(\vec{r}, \vec{r}', \varepsilon)$ to be a function of $\vec{r}$. Then, $\mathbf{G}_0(\vec{r}, \vec{r}', \varepsilon)$ are found to be a linear combination of the solutions given by Eq. (5) and the outgoing solutions (so-called irregular solutions) given by Eq. (7). Furthermore,

by taking account of the cusp condition of the Green function at $r = r'$, it is easy to derive

$$
\mathbf{G}_0(\vec{r},\vec{r}',\varepsilon) = \frac{2}{i(k_+ + k_-)}
$$
$$
\times \begin{cases} \sum_{m\alpha} k_\alpha |\psi_{\varepsilon m\alpha}^{\text{out}}\rangle\langle\psi_{\varepsilon m\alpha}| e^{-i(m+\frac{1}{2})\pi} & \text{for } r > r', \\ \sum_{m\alpha} k_\alpha |\psi_{\varepsilon m\alpha}\rangle\langle\psi_{\varepsilon m\alpha}^{\text{out}}| e^{i(m+\frac{1}{2})\pi} & \text{for } r < r'. \end{cases}
$$
(14)

Using Eqs. (14) and (10), one arrives at this general expression for the scattering coefficients:

$$
C(m\alpha, m'\alpha') = \left[\delta_{mm'}\delta_{\alpha\alpha'} + \frac{2k_{\alpha'}}{i(k_+ + k_-)} \langle\psi_{\varepsilon m'\alpha'}|\mathbf{t}|\psi_{\varepsilon m\alpha}\rangle \right]
$$
$$
\times \sqrt{\frac{k_\alpha}{k_{\alpha'}}} e^{-i(m'+\frac{1}{2})\pi}.
$$
(15)

D. Residual resistivity tensor

Using the Kubo linear response formalism [22], we can show that the components of the resistivity tensor $\rho_{\gamma\gamma'}$ measuring the potential drop in direction γ after applying an electric field in direction γ' in the dc limit $\omega \to 0$ are given in terms of the scattering solution $\varphi_{\varepsilon m\alpha}$ by

$$
\rho_{\gamma\gamma'} = \lim_{\omega\to 0} \frac{\pi\omega}{Sn_e^2 e^2} \sum_{i,j} \delta(\varepsilon_j - \varepsilon_i - \hbar\omega)(f_i - f_j)
$$
$$
\times \langle\varphi_i|m^* v_\gamma|\varphi_j\rangle\langle\varphi_j|m^* v_{\gamma'}|\varphi_i\rangle,
$$
(16)

where $\gamma, \gamma' \in \{x, y\}$, the indices i, j stand each for (ε, m, α), n_e is the surface electronic density, S denotes the area of the surface, e is the electron charge, and $f_i = \theta(\varepsilon_F - \varepsilon_i)$ is the occupation number for the energy level ε_i at $T = 0$ K. Here, n_e is related to the Fermi wave numbers of the two bands, k_{F+} and k_{F-}, by

$$
n_e = \frac{1}{4\pi}(k_{F+}^2 + k_{F-}^2),
$$
(17)

and the factor $1/S$ in Eq. (16) may be regarded as representing the impurity number density, n_i, if n_i is low enough. Also, one needs in Eq. (16) the relativistic velocity operator, i.e.,

$$
\begin{cases} v_x = -i\frac{\hbar}{m^*}\frac{\partial}{\partial x} + \frac{\hbar}{m^*}k_{\text{so}}\sigma_y, \\ v_y = -i\frac{\hbar}{m^*}\frac{\partial}{\partial y} - \frac{\hbar}{m^*}k_{\text{so}}\sigma_x. \end{cases}
$$

In addition to the prefactor ω, the summation over states i and j in Eq. (16) gives rise to another factor ω, since ε_i must satisfy the condition $\varepsilon_F - \hbar\omega \leqslant \varepsilon_i \leqslant \varepsilon_F$. In spite of this, the right-hand side of Eq. (16) takes a finite limiting value in the limit of $\omega \to 0$, since the matrix elements $\langle\varphi_i|m^* v_\gamma|\varphi_j\rangle$ evaluated for the asymptotic scattering region ($r \to \infty$) diverge as $1/\omega$ in the limit of $\omega \to 0$, as will be demonstrated in Appendix A.

The resistivity tensor is related to the energy dissipation P in the system per unit time by

$$
P = \sum_{\gamma,\gamma'} \rho_{\gamma\gamma'} J_\gamma^* J_{\gamma'},
$$
(18)

where J_γ denotes the 2D current density in the γ direction. By inserting the matrix elements of the momentum operators in the limit of $\omega \to 0$ given in Appendix A into Eq. (16),

one can derive the most general expression for the diagonal components of the resistivity tensor,

$$
\rho_{\gamma\gamma} = \frac{\hbar k_{\text{FM}}^2}{8\pi Sn_e^2 e^2} \sum_{m\alpha, m'\alpha'} \left| (\delta_{m',m+1} \pm \delta_{m',m-1})\delta_{\alpha\alpha'} \right.
$$
$$
+ \sum_{l\alpha''} C(m\alpha, l\alpha'')C^*(m'\alpha', l+1\alpha'')
$$
$$
\left. \pm \sum_{l\alpha''} C(m\alpha, l\alpha'')C^*(m'\alpha', l-1\alpha'') \right|^2,
$$
(19)

where $k_{\text{FM}} = k_M(\varepsilon_F)$ and the plus and minus signs correspond to ρ_{xx} and ρ_{yy}, respectively. In deriving Eq. (19), we replaced in (16) the sum $\sum_i$ over discrete states by $\frac{1}{2\pi}\sum_{m=-\infty}^{+\infty}\sum_{\alpha=\pm}\int_0^{+\infty} k_\alpha dk_\alpha$. The scattering coefficients $C(m\alpha, m'\alpha')$ are implicitly energy dependent. After integrating over k_α, these coefficients will be taken at the Fermi level, ε_F. In the case of the absence of the impurity, the resistivity vanishes since the scattering coefficients are given in this case simply by $C(m\alpha, m'\alpha') = \delta_{mm'}\delta_{\alpha\alpha'}e^{-i(m+1/2)\pi}$.

If we assume that the impurity has no on-site SO coupling and also that it has a magnetic moment perpendicular to the surface, then the t matrix is diagonal in spin space,

$$
\mathbf{t} = \begin{pmatrix} t_{\uparrow\uparrow} & 0 \\ 0 & t_{\downarrow\downarrow} \end{pmatrix},
$$
(20)

i.e., spin-up and spin-down electrons scatter differently at the impurity. However, the scattering is not spin conserving because the spin of the Rashba electrons lies in the plane and the t matrix is no longer diagonal in that spin frame of reference. Furthermore, if the impurity potential is cylindrical, the orbital momentum representation of $t_{\sigma\sigma}$ with $\sigma \in \{\uparrow, \downarrow\}$ reads

$$
t_{\sigma\sigma}(\vec{r},\vec{r}') = \frac{1}{2\pi}\sum_m e^{im\phi} t_{\sigma\sigma,m}(r,r')e^{-im\phi'}.
$$
(21)

In this case, as seen from Eq. (15), the scattering coefficient $C(m\alpha, m'\alpha')$ becomes diagonal with respect to m and m', and the expression for the resistivity, given by Eq. (19), is further simplified as

$$
\rho_{\gamma\gamma} = \frac{\hbar k_{\text{FM}}^2}{8\pi Sn_e^2 e^2} \sum_{m\alpha, m'=m\pm 1 \, \alpha'}
$$
$$
\times \left| \delta_{\alpha\alpha'} + \sum_{\alpha''} C(m\alpha, m\alpha'')C^*(m'\alpha', m'\alpha'') \right|^2.
$$
(22)

Obviously, the two diagonal components, ρ_{xx} and ρ_{yy}, are identical in this case.

E. In the limit of $k_{\text{so}} = 0$

Here, we consider the limit of $k_{\text{so}} \to 0$ to derive the expression of the residual resistivity induced by a localized impurity for the 2D free-electron gas without the Rashba SO term. For this purpose, it is better to choose energy ϵ, orbital angular momentum m, and spin index σ as the quantum numbers for the description of scattering states, where the spin-quantization axis is chosen as the z axis as in previous

sections. Namely, instead of Eqs. (6) and (7), we employ

$$\tilde{\psi}_{\varepsilon m \sigma}^{\text{in}}(\vec{r}) = \frac{1}{2} e^{-\frac{2m+1}{4}\pi i} H_m^{(2)}(kr) e^{im\phi} |\sigma\rangle, \qquad (23)$$

and

$$\tilde{\psi}_{\varepsilon m \sigma}^{\text{out}}(\vec{r}) = \frac{1}{2} e^{\frac{2m+1}{4}\pi i} H_m^{(1)}(kr) e^{im\phi} |\sigma\rangle, \qquad (24)$$

as the incident and scattered electron wave functions, where $k = \sqrt{2m^*\varepsilon}/\hbar$, $|\uparrow\rangle = (1,0)$, and $|\downarrow\rangle = (0,1)$.

Then, the wave function of an incident electron with quantum state (ε, m, σ) scattering elastically from a noncylindrical impurity potential placed at the origin is expressed as

$$\tilde{\varphi}_{\varepsilon m \sigma}(\vec{r}) = \tilde{\psi}_{\varepsilon m \sigma}^{\text{in}}(\vec{r}) + \sum_{m',\sigma'} \tilde{C}(m\sigma, m'\sigma') \tilde{\psi}_{\varepsilon m'\sigma'}^{\text{out}}(\vec{r}). \qquad (25)$$

By following the same procedure, we can easily show that the resistivity tensor for the present case with $\alpha_{\text{so}} = 0$ is given exactly in the same form as Eq. (19), except that $k_{\text{F}\alpha}$ is replaced by $k_{\text{F}} = \sqrt{2m^*\varepsilon_{\text{F}}}/\hbar$, the scattering coefficients of the type $C(m\alpha, m'\alpha')$ are replaced by $\tilde{C}(m\sigma, m'\sigma')$, and further the summation over band indices is replaced by the one over spin indices.

Furthermore, if the t matrix is diagonal with respect to electron spin and the impurity potential has cylindrical symmetry, we can derive a more simplified expression corresponding to Eq. (22),

$$\rho_{\gamma\gamma} = \frac{\hbar k_{\text{F}}^2}{8\pi S n_e^2 e^2} \sum_{m,m'=m\pm 1,\sigma} |1 + \tilde{C}(m\sigma, m\sigma)\tilde{C}^*(m'\sigma, m'\sigma)|^2, \qquad (26)$$

where it should be noted that in contrast to the Rashba electrons with a finite α_{so}, the spin-flip scattering does not occur in the present case. The scattering coefficient in the above equation can be expressed by using the phase shift as

$$\tilde{C}(m\sigma, m\sigma) = e^{-(m+\frac{1}{2})\pi i + 2\delta_m(\varepsilon,\sigma)i}. \qquad (27)$$

By inserting this expression into Eq. (26), we obtain finally

$$\rho_{\gamma\gamma} = \frac{2\hbar}{S n_e e^2} \sum_{\sigma=\uparrow\downarrow} \sum_{m=-\infty}^{+\infty} \sin^2[\delta_{m+1}(\varepsilon_{\text{F}},\sigma) - \delta_m(\varepsilon_{\text{F}},\sigma)], \qquad (28)$$

where we used the relation $k_{\text{F}}^2 = 2\pi n_e$. This is a modification of Friedel's result [26] for the residual resistivity of a single impurity in a 3D electron gas [see Eq. (1)] to the case of an impurity in a 2D electron gas without the Rashba-type SO term. The only difference is the scattering phase space of momentum transfer in the field direction, which is larger in the 3D case than in 2D, and this is taken care of in Eq. (1) by the multiplicity $\ell + 1$ of each angular momentum component.

F. s-wave scatterer

In this section, we will consider the scattering of Rashba electrons by an impurity whose spatial extent is much smaller than the Fermi wave length. For such a scatterer, one may be able to employ the δ-function approximation for the t matrix,

$$t_{\sigma\sigma'}(\vec{r}, \vec{r}') = \delta(\vec{r})\delta(\vec{r}') \, t_{\sigma\sigma'}(\varepsilon). \qquad (29)$$

It should be noted that within this s-wave approximation, only $\psi_{\varepsilon,m=0,\alpha}(\vec{r})$ having $J_0(k_\alpha r)$ for its up-spin component and $\psi_{\varepsilon,m=-1,\alpha}(\vec{r})$ having $J_0(k_\alpha r)$ for its down-spin component

make nonzero contributions to the matrix elements of the t matrix, $\langle \psi_{\varepsilon m'\alpha'} | \mathbf{t} | \psi_{\varepsilon m\alpha} \rangle$, since $J_m(0)$ vanishes for $m > 0$.

We aim to derive the general expression of the impurity resistivity when the t matrix is given by Eq. (29). First, we note that by using Eq. (15), the scattering coefficients $C(m\alpha, m'\alpha')$ for m and m' equal to 0 or -1 are given by

$$C(0\alpha, 0\alpha') = \frac{1}{i}\delta_{\alpha\alpha'} - \frac{\sqrt{k_\alpha k_{\alpha'}}}{2k_{\text{M}}} t_{\uparrow\uparrow},$$

$$C(-1\alpha, -1\alpha') = i\delta_{\alpha\alpha'} + \frac{\sqrt{k_\alpha k_{\alpha'}}}{2k_{\text{M}}} s(\alpha)s(\alpha') t_{\downarrow\downarrow},$$

$$\qquad\qquad\qquad\qquad\qquad\qquad\qquad\qquad (30)$$

$$C(0\alpha, -1\alpha') = \frac{\sqrt{k_\alpha k_{\alpha'}}}{2ik_{\text{M}}} s(\alpha') t_{\downarrow\uparrow},$$

$$C(-1\alpha, 0\alpha') = \frac{\sqrt{k_\alpha k_{\alpha'}}}{2ik_{\text{M}}} s(\alpha) t_{\uparrow\downarrow},$$

where $s(\alpha)$ is defined by $s(\pm 1) = \mp 1$ and the energy argument for the t matrix is omitted for simplicity. For m and m' larger than 0 or smaller than -1, we have

$$C(m\alpha, m'\alpha') = \delta_{mm'}\delta_{\alpha\alpha'} e^{-i(m+\frac{1}{2})\pi}. \qquad (31)$$

The expression of the impurity resistivity can be obtained by inserting Eqs. (30) and (31) into Eq. (19), where 12 pairs of (m, m') make a nonvanishing contribution to the resistivity. After a lengthy calculation, one obtains

$$\rho_{\gamma\gamma} = \frac{\hbar k_{\text{FM}}^2}{2\pi S n_e^2 e^2}\left[\sum_{\sigma,\sigma'} |t_{\sigma\sigma'}|^2 - \left(\frac{k_{\text{so}}}{k_{\text{FM}}}\right)^2 (M \mp N)\right], \qquad (32)$$

with

$$M \equiv \text{Re}(t_{\uparrow\uparrow}^* t_{\downarrow\downarrow}) + \frac{1}{2}(|t_{\uparrow\downarrow}|^2 - |t_{\downarrow\uparrow}|^2)^2, \qquad (33)$$

$$N \equiv \text{Re}(t_{\uparrow\downarrow}^* t_{\downarrow\uparrow}) - \frac{1}{2}\text{Re}$$
$$\times [(t_{\uparrow\uparrow}^* - t_{\downarrow\downarrow}^*) \, t_{\downarrow\uparrow} - (t_{\uparrow\uparrow} - t_{\downarrow\downarrow}) \, t_{\uparrow\downarrow}^*]^2, \qquad (34)$$

where the t matrix should be evaluated at the Fermi energy and the negative and positive signs in Eq. (32) correspond to ρ_{xx} and ρ_{yy}, respectively. In deriving the above equations, we have used the general relation for the t matrix (optical theorem), $\mathbf{t} - \mathbf{t}^\dagger = -i \, \mathbf{t}\mathbf{t}^\dagger$, implying in the case of a 2×2 matrix that

$$\text{Im } t_{\uparrow\uparrow} = -\frac{1}{2}(|t_{\uparrow\uparrow}|^2 + |t_{\downarrow\uparrow}|^2),$$

$$\text{Im } t_{\downarrow\downarrow} = -\frac{1}{2}(|t_{\downarrow\downarrow}|^2 + |t_{\uparrow\downarrow}|^2),$$

$$t_{\uparrow\downarrow}^* - t_{\downarrow\uparrow} = i(t_{\uparrow\uparrow} t_{\uparrow\downarrow}^* + t_{\downarrow\downarrow}^* t_{\downarrow\uparrow}).$$

Because of the above relations, M and N in Eqs. (33) and (34) may be expressed in many apparently different but equivalent ways.

III. RESULTS AND DISCUSSIONS

As mentioned above, we investigate the example of Fe adatoms on an Au(111) surface with an area $S = 1$ m^2 (unit area), considering the scattering of the Shockley surface states of Au(111) at the adatom. We assume that the impurity has no on-site SO coupling term. Furthermore, we will consider only cylindrical potentials. In the case where the magnetic moment of the impurity is oriented in the z direction, the t matrix can be expressed by Eqs. (20) and (21). Since
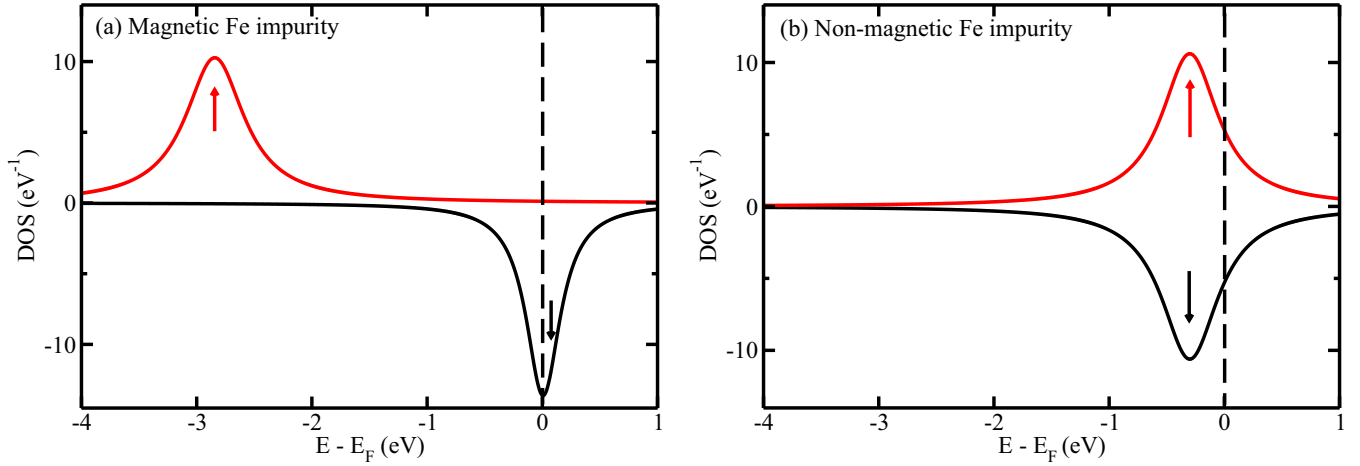
FIG. 1. Local density of states of an Fe adatom deposited on a Au(111) surface described by a Lorentzian model wherein the broadening is induced by hybridization effects among the electronic states of the impurity with those of the substrate. Two cases are considered: (a) a magnetic vs (b) a nonmagnetic impurity. After defining the phase shifts at the Fermi energy in the magnetic case, the phase shifts in the nonmagnetic case are derived considering the same charge for both types of impurities.

the characteristic wavelengths of the Rashba electrons at ε_F corresponding to k_{F+} and k_{F-} are much larger than the impurity size, we can proceed with the so-called s-wave approximation (see Sec. II F). Indeed, the wavelengths $\lambda_{F+} = 2\pi/0.192 = 32.7$ Å, $\lambda_{F-} = 2\pi/0.167 = 37.6$ Å are large considering $k_{so-} = -0.0125$ Å^{-1}, with parameters taken from Ref. [4]. The advantages of this approximation are the fast numerical evaluation of the scattering coefficients and an easy tracking of the impact of scattering on the resistivity. The connection to the phase shift will be needed in the upcoming discussion and is given via $t_{\sigma\sigma}(\varepsilon) = i\,(e^{2i\delta_0(\varepsilon,\sigma)} - 1)$, which are the diagonal elements of the t matrix in spin space [see Eq. (20)].

The s-wave approximation has been used numerous times for the interpretation of scanning-tunneling-microscopy-based experiments [28–31]. This was done in the context of standing waves on a Cu(111) surface [20] or Au(111) surface [32] and confined electronic states in corrals of Fe or Co adatoms deposited on a Cu(111) surface [33,34]. For Fe adatoms on a Cu(111) surface, good fits to the experimental features were obtained with a phase shift of $\pi/2$, but a better agreement was found with a phase shift of $i\infty$, which would correspond to maximally absorbing adatoms (black dots) [34]. In the latter case, the overall scattering amplitude reduces by a factor of 2 compared to a phase shift of $\pi/2$.

We follow a description similar to the one of Heller *et al.* [34], but considering a phase shift of $\pi/2$ in the minority-spin channel. The majority-spin channel is considered fully occupied in the magnetic case and thus the corresponding phase shift is set to π. These assumptions were used in Ref. [21] and are confirmed by our *ab initio* simulations based on density functional theory as implemented in the Korringa-Kohn-Rostoker Green-function method [35]. From these calculations, we learned that the easy axis of the Fe magnetic moment is out of plane. The adatom local density of states (LDOS) is characterized by a resonance close to ε_F in the minority-spin channel and the exchange splitting between the majority-spin and minority-spin resonances is about 2.8 eV. The broadening of the resonances in the magnetic case is 0.6 eV in the majority-spin channel and 0.4 eV in

the minority-spin channel, while in the nonmagnetic case it is considered to be 0.6 eV. Therefore, we assume that the LDOS considered in our model follows the Lorentzian shapes depicted in Fig. 1(a). We note that in our scheme based on linear response theory, only the phase shift at the Fermi energy is essential.

In order to evaluate the impact of magnetism on the residual resistivity, we consider a nonmagnetic Fe adatom and use charge conservation in order to guess the appropriate parameters. The spin-dependent charge N_σ of the impurity is given by $\frac{1}{\pi}\,\delta_0(\varepsilon_F, \sigma)$ with the Friedel sum rule. Charge conservation imposes then that in the nonmagnetic case, $\delta_0(\varepsilon_F, \uparrow) = \delta_0(\varepsilon_F, \downarrow) = \frac{3\pi}{4}$, which leads to the LDOS plotted in Fig. 1(b).

Considering the approximations mentioned above, one can investigate the residual resistivity for both cases: magnetic and nonmagnetic Fe adatoms. To start our analysis, we consider a magnetic moment pointing perpendicular to the surface. Also, to make our study general, we explore different SO coupling strengths, which then would correspond to the deposition of the impurities on different substrates. To make these types of investigations consistent with each other, the energy of the highest occupied state of the Rashba electron gas measured from the bottom of the energy-dispersion curve, $\varepsilon_F^{\text{Rashba}} = \varepsilon_F + \frac{\hbar^2}{2m^*}k_{so}^2$, is set to a constant, 480 meV for the case of the Au(111) surface state characterized by an effective mass $m^* = 0.255 m_e$ [4]. By changing k_{so}, ε_F is modified such that $\varepsilon_F^{\text{Rashba}}$ does not vary.

By inserting $t_{\uparrow\uparrow} = i(e^{i\delta_0(\varepsilon_F, \uparrow)} - 1)$, $t_{\downarrow\downarrow} = i(e^{i\delta_0(\varepsilon_F, \downarrow)} - 1)$, and $t_{\uparrow\downarrow} = t_{\downarrow\uparrow} = 0$ into Eq. (32), we obtain, as the resistivity induced by a magnetic adatom with its magnetic moment pointing to the normal direction,

$$\rho_{\gamma\gamma} = \frac{2\hbar k_{\text{FM}}^2}{\pi S n_e^2 e^2}\left[\sin^2(\delta_\uparrow) + \sin^2(\delta_\downarrow) \right.$$
$$\left. - \left(\frac{k_{so}}{k_{\text{FM}}}\right)^2 \sin(\delta_\uparrow)\sin(\delta_\downarrow)\cos(\delta_\uparrow - \delta_\downarrow) \right], \quad (35)$$

where $\delta_\uparrow$ and $\delta_\downarrow$ are abbreviations of $\delta_0(\varepsilon_F, \uparrow)$ and $\delta_0(\varepsilon_F, \downarrow)$, respectively. Thus, for the present nonmagnetic adatom with $\delta_\uparrow = \delta_\downarrow = \frac{3\pi}{4}$,

$$\rho_{\gamma\gamma} = \frac{2\hbar k_{FM}^2}{\pi S n_e^2 e^2}\left[1 - \frac{1}{2}\left(\frac{k_{so}}{k_{FM}}\right)^2\right], \quad (36)$$

while for the present magnetic adatom with $\delta_\uparrow = \pi$ and $\delta_\downarrow = \pi/2$, we simply have

$$\rho_{\gamma\gamma} = \frac{2\hbar k_{FM}^2}{\pi S n_e^2 e^2}, \quad (37)$$

where k_{FM} and n_e are related to ε_F^{Rashba}, which is kept constant in the numerical calculation, by $k_{FM}^2 = 2m^*\varepsilon_F^{Rashba}/\hbar^2$ and $n_e = \frac{m^*\varepsilon_F^{Rashba}}{\pi\hbar^2} + \frac{k_{so}^2}{2\pi}$. The latter leads to a quadratic decrease of the prefactor $\frac{2\hbar k_{FM}^2}{\pi S n_e^2 e^2}$ and thus of the residual resistivity with respect to k_{so}^2. This simply indicates that the more available electrons, the more conducting the system becomes.

The intriguing dependence of n_e on the SO coupling strength can be traced back to the particular behavior of the density of states of the Rashba electron gas, which is characterized by two regimes induced by SO and defined by the two regions of the energy-dispersion curve that show a crossing at $k = 0$ [see Eq. (4)]. At energies below the crossing, the corresponding density of states follows a quasi-one-dimensional behavior where a van Hove singularity occurs at the bottom of the bands. Above the crossing, the density of states is a constant, as expected for a 2D electron gas. By increasing the SO coupling strength, the quasi-one-dimensional region becomes larger in order to keep ε_F^{Rashba} constant, which leads to the quadratic dependence of n_e on k_{so} and explains the strong drop of the residual resistivity when increasing the SO coupling strength.

The latter can be observed in Fig. 2, where the longitudinal residual resistivity as a function of SO is depicted. The transversal residual resistivity is not shown since it is zero for the two cases considered: magnetic (out-of-plane moment) and nonmagnetic adatoms. Interestingly, magnetism and SO coupling strength have the opposite impact on the residual resistivity. This holds for spin-dependent phase shifts that con-

serve the number of electrons N of the impurity after spin polarization. Indeed, as may be seen from Eq. (35), in contrast to magnetism, SO coupling tends to decrease the resistivity. The largest resistivity is found when the SO interaction is switched off, which would correspond to the case of a Cu(111) surface. Here the residual resistivity is independent from the magnetic nature of the adatom, as can be deduced from Eq. (35),

$$\rho_{\gamma\gamma} = \frac{4\hbar}{S n_e e^2}[\sin^2(\delta_\uparrow) + \sin^2(\delta_\downarrow)]. \quad (38)$$

Now, we address the dependence of the residual resistivity on the magnetism of the impurity by analyzing the different scattering processes allowed at the Fermi surface. The possible elastic-scattering processes can be found by evaluating the probability for an electron scattering from a state $|\psi_{\vec{k}\alpha}\rangle$ to a state $|\psi_{\vec{k}'\alpha'}\rangle$:

$$P_{\vec{k}\vec{k}'}^{\alpha\alpha'} = \frac{2\pi}{\hbar}|\langle\psi_{\vec{k}'\alpha'}|\mathbf{t}|\psi_{\vec{k}\alpha}\rangle|^2 \,\delta(\varepsilon_{\vec{k}\alpha} - \varepsilon_{\vec{k}'\alpha'}), \quad (39)$$

where $\psi_{\vec{k}\alpha}$ are given by Eq. (3) and α is the band index. If the impurity is nonmagnetic, the diagonal elements of the t matrix in spin space are equal: $t_{\uparrow\uparrow} = t_{\downarrow\downarrow} = t$. In this case, the electron scattering probabilities are given by

$$P_{\vec{k}\vec{k}'}^{\alpha\alpha'} = \frac{\pi}{2\hbar}|t|^2[1 + \alpha\alpha'\cos(\phi_{\vec{k}} - \phi_{\vec{k}'})]\,\delta(\varepsilon_{\vec{k}\alpha} - \varepsilon_{\vec{k}'\alpha'}), \quad (40)$$

where $\alpha\alpha'$ equals 1 for intraband scattering transitions ($\alpha = \alpha'$) or -1 for interband transitions ($\alpha \neq \alpha'$). This equation shows that interband and intraband transitions flipping the spin are not allowed since, in these cases, $\phi_{\vec{k}} - \phi_{\vec{k}'} = \pi$ with $\alpha\alpha' = 1$ and $\phi_{\vec{k}} - \phi_{\vec{k}'} = 0$ with $\alpha\alpha' = -1$, respectively [see Fig. 3(a)].

In the case of a magnetic impurity with a moment perpendicular to the surface, the t matrix is given by Eq. (20) and all transitions are allowed, even those leading to a spin flip, as depicted in Fig. 3(b). Here the electron scattering probabilities are

$$P_{\vec{k}\vec{k}'}^{\alpha\alpha'} = \frac{2\pi}{\hbar}|t_{\uparrow\uparrow} + \alpha\alpha' t_{\downarrow\downarrow}e^{i(\phi_{\vec{k}} - \phi_{\vec{k}'})}|^2 \,\delta(\varepsilon_{\vec{k}\alpha} - \varepsilon_{\vec{k}'\alpha'}), \quad (41)$$

which is different from zero independently from the value of $\phi_{\vec{k}} - \phi_{\vec{k}'}$. This is due to the magnetic moment of the impurity which breaks the time-reversal symmetry. Thus, there are more scattering possibilities than in the nonmagnetic case, and therefore for magnetic impurities a higher residual resistivity is expected as to nonmagnetic impurities, in line with Fig. 2.

Up to now, the magnetic moment was considered perpendicular to the surface plane. To generalize our study, we explore the impact of arbitrary orientations, $\hat{e}_{\vec{M}}$, of the impurity moment $\vec{M}$ on the residual resistivity. The resistivity is a tensor and, contrary to the case of an out-of-plane magnetic orientation, its off-diagonal elements become finite for arbitrary magnetization directions, giving rise to the AMR and PHE. To tackle this problem, we rotate the impurity magnetic moment pointing initially normal to the surface plane, $\hat{e}_z$, by means of the conventional 3×3 rotation matrices, $\mathcal{R} \in SO(3)$, by a polar angle $\theta_{\vec{M}}$ between the direction of the magnetic moment and the z axis and an azimuthal angle $\phi_{\vec{M}}$, $\hat{e}_{\vec{M}} = \mathcal{R}_z(\phi_{\vec{M}})\mathcal{R}_y(\theta_{\vec{M}})\hat{e}_z$. This translates to a unitary transformation of the t matrix in spin
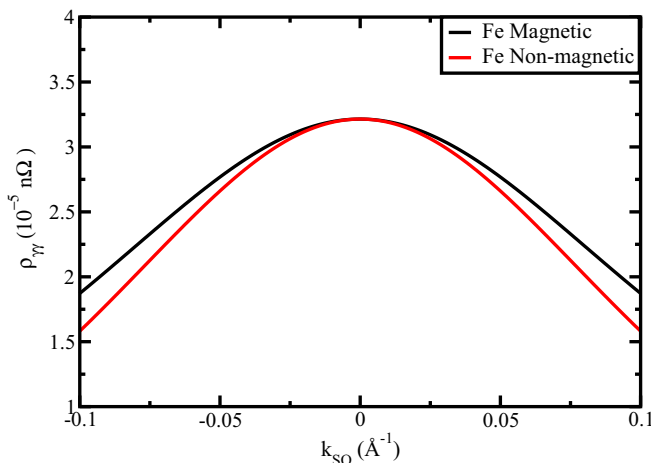

FIG. 2. Evolution of the diagonal components of the resistivity tensor as a function of the spin-orbit wave-vector length (k_{so}) for a magnetic and a nonmagnetic Fe impurity.

(a) Non-magnetic impurity

(b) Impurity moment along z

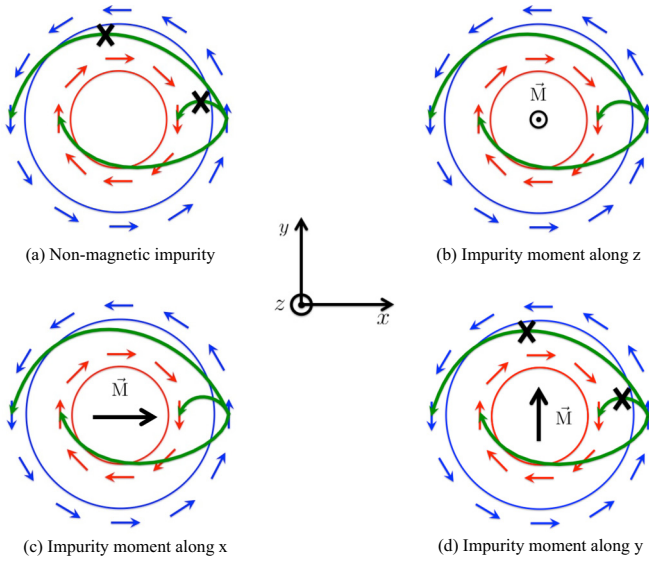(c) Impurity moment along x

(d) Impurity moment along y

FIG. 3. Fermi-surface scattering processes of Rashba electrons at a (a) nonmagnetic impurity, (b) magnetic impurity with an out-of-plane magnetic moment, (c) in-plane magnetic moment pointing along the x direction, and (d) along the y direction. The transitions between circles with different colors are interband transitions, while transitions between circles with the same color are intraband transitions. The green arrows indicate the connection between the initial and final state. The crosses indicate prohibited scattering processes, while the black arrows at the center of the Fermi contours represent the direction of the impurity magnetic moment.

space, $\mathbf{t}'(\vec{r},\vec{r}') = \mathbf{U}(\theta_{\vec{M}},\phi_{\vec{M}})\,\mathbf{t}(\vec{r},\vec{r}')\,\mathbf{U}^\dagger(\theta_{\vec{M}},\phi_{\vec{M}})$. $\mathbf{U}(\theta_{\vec{M}},\phi_{\vec{M}}) = \mathbf{U}(\mathcal{R}_z,\phi_{\vec{M}})\mathbf{U}(\mathcal{R}_y,\theta_{\vec{M}})$ are the conventional rotation operators in SU(2), whose representation in terms of a 2×2 matrix is given by $\mathbf{U}(\mathcal{R}_\gamma,\beta) = \cos(\beta/2) \otimes \mathbb{1}_2 - i\sin(\beta/2)\boldsymbol{\sigma}_\gamma$. The t matrix for an arbitrary rotation angle of the moment can then be expressed in terms of the spin-diagonal elements, $t_{\uparrow\uparrow}$ and $t_{\downarrow\downarrow}$, describing the out-of-plane moment [see Eq. (20)] as

$$\mathbf{t} = \tfrac{1}{2}(t_{\uparrow\uparrow} + t_{\downarrow\downarrow}) \otimes \mathbb{1}_2 + \tfrac{1}{2}(t_{\uparrow\uparrow} - t_{\downarrow\downarrow})\,\vec{\sigma}\cdot\hat{e}_{\vec{M}}. \quad (42)$$

For given values of $\{\theta_{\vec{M}},\phi_{\vec{M}}\}$, the matrix $\mathbf{t}'(\vec{r},\vec{r}')$ might have nonzero off-diagonal components. We note that we chose to define the azimuthal angle with respect to the x axis being the direction of the perturbing current.

The longitudinal and transversal components of the residual resistivity in the whole phase space of rotation angles is depicted in Figs. 4(a) and 4(b). The images exhibit a clearly visible angular dependence. The anisotropy of the resistivity is of the order of 10^{-8} nΩ. In the case of the longitudinal resistivity, this anisotropy modifies the isotropic contribution of the longitudinal resistivity, which is of the order of 3.180×10^{-5} nΩ by about $\pm 0.14\%$. Since for the transversal resistivity the isotropic contribution is exactly zero, the anisotropy is given as absolute values.

Now we turn to the analysis of the angular dependence of the resistivity anisotropy. This is different from the functional form for such a general angular dependence available in the literature, where the magnetization is lying in plane [36]. Therefore, to simplify our analysis, we focus first on the particular orientation of the magnetic moment along the x

direction. There, the t matrix given by Eq. (42) is expressed as

$$\mathbf{t}' = \frac{1}{2}\begin{pmatrix} t_{\uparrow\uparrow} + t_{\downarrow\downarrow} & t_{\uparrow\uparrow} - t_{\downarrow\downarrow} \\ t_{\uparrow\uparrow} - t_{\downarrow\downarrow} & t_{\uparrow\uparrow} + t_{\downarrow\downarrow} \end{pmatrix}, \quad (43)$$

where $t_{\uparrow\uparrow}$ and $t_{\downarrow\downarrow}$ are the upper and lower diagonal components of the t matrix when the magnetic moment points along the z direction. As we will discuss below, this gives rise to a nonzero off-diagonal contribution in the resistivity tensor and contributes to the PHE even without spin-orbit contribution at the impurity site. When the magnetic moment is in the surface plane ($\theta_{\vec{M}} = \frac{\pi}{2}$), Figs. 4(c) and 4(d) show the behavior of the diagonal and off-diagonal components of the resistivity tensor, respectively, as a function of the azimuthal angle $\phi_{\vec{M}}$. The trace of the resistivity tensor is conserved under these azimuthal rotations ($\rho_{xx} + \rho_{yy} = \text{const}, \forall\, \phi_{\vec{M}}$), while the off-diagonal components are related by $\rho_{xy} = \rho_{yx}$.

The diagonal components of the resistivity tensor [Fig. 4(c)] can be fitted with the AMR functional form given by Thompson *et al.* [36]: $\rho_{\gamma\gamma} = \rho_\perp + (\rho_\parallel - \rho_\perp)\cos^2(\phi_{\vec{M}})$, where $\rho_\parallel$ and $\rho_\perp$ define the residual resistivities when the moment is, respectively, parallel and perpendicular to the current. In our particular case, the current is pointing along the x direction, thus $\rho_\parallel = \rho_{xx}(\phi_{\vec{M}} = 0)$ and $\rho_\perp = \rho_{xx}(\phi_{\vec{M}} = \frac{\pi}{2})$. It turns out that $(\rho_\parallel - \rho_\perp)$, i.e., the maximal value of the AMR, is a positive quantity as expected for a Rashba electron gas [37]. This can be explained by analyzing the different scattering processes on the Fermi surface when the impurity magnetic moment is in plane [see Figs. 3(c) and 3(d)]. As done previously, the idea is to evaluate the scattering probabilities for an arbitrary rotation of the magnetic moment [see Eq. (42)]. Here we provide the results obtained for scattering processes from $\phi_{\vec{k}} = 0$ to $\phi_{\vec{k}'} = 0$ or π. If $\phi_{\vec{k}'} - \phi_{\vec{k}} = 0$, only interband transitions, i.e., $\alpha \neq \alpha'$, can contribute,

$$P_{\vec{k}\vec{k}'}^{\alpha\alpha'} = \frac{2\pi}{\hbar}|t_{\uparrow\uparrow} - t_{\downarrow\downarrow}|^2(\cos^2\theta_{\vec{M}} + \sin^2\theta_{\vec{M}}\cos^2\phi_{\vec{M}}) \\ \times \delta(\varepsilon_{\vec{k}\alpha} - \varepsilon_{\vec{k}'\alpha'}), \quad (44)$$

which is zero if the moment points along the y direction. This is the same result obtained for intraband scattering probability, $P_{\vec{k}\vec{k}'}^{\alpha\alpha}$, when $\phi_{\vec{k}'} - \phi_{\vec{k}} = \pi$. For the latter angle configuration, the interband scattering probability is nonzero independently from the rotation angle of the moment,

$$P_{\vec{k}\vec{k}'}^{\alpha\alpha'} = \frac{2\pi}{\hbar}|t_{\uparrow\uparrow} + t_{\downarrow\downarrow} + \alpha(t_{\uparrow\uparrow} - t_{\downarrow\downarrow})\sin\theta_{\vec{M}}\sin\phi_{\vec{M}}|^2 \\ \times \delta(\varepsilon_{\vec{k}\alpha} - \varepsilon_{\vec{k}'\alpha'}). \quad (45)$$

To summarize, when the magnetic moment points along the current direction (x direction), the backscattering is due to interband and intraband scattering. However, when the magnetic moment is perpendicular to the current direction, the backscattering is only originating from interband transitions, which induces a smaller residual resistivity and therefore gives a positive maximal value of the AMR, i.e., $\rho_\parallel > \rho_\perp$. Similar scattering processes are possible when the moment points along the x direction or the z direction, which explains that the resistivities are the same for both magnetic orientations.

The off-diagonal components of the resistivity tensor [Fig. 4(d)] could be fitted with the PHE functional form [36] $\rho_{\gamma\gamma'} = (\rho_\parallel - \rho_\perp)\cos(\phi_{\vec{M}})\sin(\phi_{\vec{M}})$. We notice that for

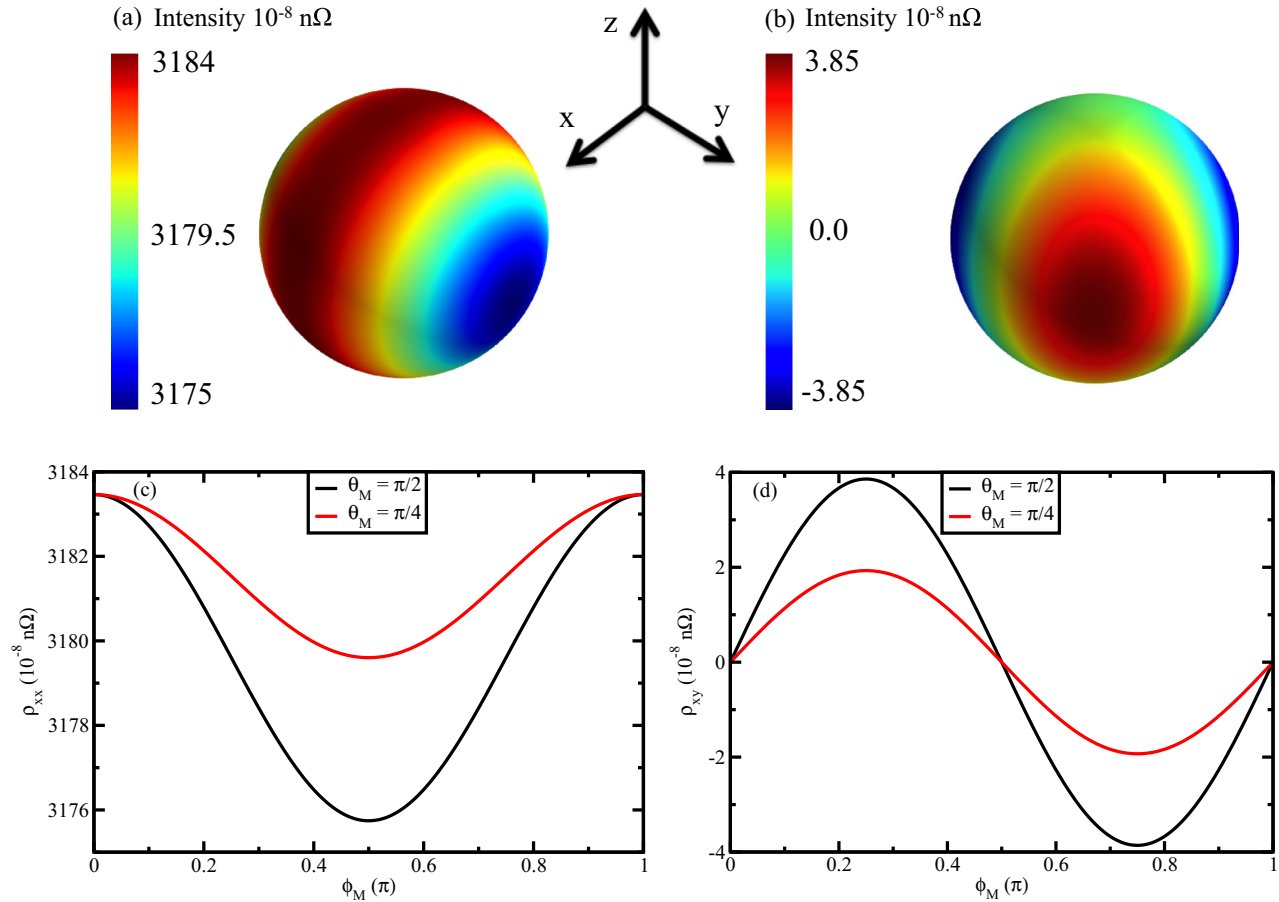FIG. 4. Evolution of the components of the residual resistivity tensor as a function of the orientation of the magnetic moment in all 4π spatial directions: (a) longitudinal component (ρ_{xx}) and (b) transversal component (ρ_{xy}). Every point on the sphere corresponds to a given orientation of the magnetic moment. Evolution of the residual resistivity tensor components while changing only $\phi_{\bar{M}}$ when the magnetic moment is pointing in-plane along the x direction: (c) longitudinal and (d) transversal component. Here we plotted the following cases: $\theta_{\bar{M}} = \frac{\pi}{2}$ (black curve) and $\theta_{\bar{M}} = \frac{\pi}{4}$ (red curve).

the considered polar angles ($\theta_{\bar{M}} = \frac{\pi}{2}, \theta_{\bar{M}} = \frac{\pi}{4}$), $\rho_{\gamma\gamma'}$ changes sign when $\phi_{\bar{M}}$ crosses $\frac{\pi}{2}$ [Fig. 4(d)]. This is accompanied by a direction switch of the Hall-like electric field originating from the PHE. The change in the sign of $\rho_{\gamma\gamma'}$ reduces the energy dissipation P given by Eq. (18) since $\rho_{\gamma\gamma}$ is always positive.

Let us go back to the general case, where the magnetic moment points in arbitrary orientations. As mentioned earlier, here we propose a phenomenological functional form for the residual resistivity. In Appendix B, we derive phenomenological functional forms for the residual resistivity tensor and show that the longitudinal and transversal parts follow a simple angular dependence:

$$\rho_{xx} = \rho_{\parallel} - (\rho_{\parallel} - \rho_{\perp}) \sin^2(\phi_{\bar{M}}) \sin^2(\theta_{\bar{M}}), \quad (46)$$

$$\rho_{xy} = (\rho_{\parallel} - \rho_{\perp}) \cos(\phi_{\bar{M}}) \sin(\phi_{\bar{M}}) \sin^2(\theta_{\bar{M}}). \quad (47)$$

These equations perfectly describe the angular dependence plotted, for instance, in Figs. 4(c) and 4(d) with the polar angle $\theta_{\bar{M}} = \frac{\pi}{2}$ (black curve) and $\theta_{\bar{M}} = \frac{\pi}{4}$ (red curve).

Alternatively, one may also derive the angular dependence of the diagonal components of the resistivity tensor directly from Eq. (32). By applying the aforementioned unitary transformations in spin space, given by Eq. (42), to the t matrix,

and substituting its matrix elements into Eq. (32), one yields the diagonal components of the resistivity. In the present case, the second terms of M and N, which are proportional to the fourth power of $t_{\sigma\sigma'}$, vanish identically and one obtains

$$\rho_{xx} = \frac{2\hbar k_{\text{FM}}^2}{\pi S n_e^2 e^2} \left[\sin^2(\delta_{\uparrow}) + \sin^2(\delta_{\downarrow}) \right.$$
$$- \left(\frac{k_{\text{so}}}{k_{\text{FM}}} \right)^2 \sin(\delta_{\uparrow}) \sin(\delta_{\downarrow}) \cos(\delta_{\uparrow} - \delta_{\downarrow})$$
$$\left. - \left(\frac{k_{\text{so}}}{k_{\text{FM}}} \right)^2 \frac{1}{2} \sin^2(\delta_{\uparrow} - \delta_{\downarrow}) \sin^2\theta_{\bar{M}} \sin^2\phi_{\bar{M}} \right], \quad (48)$$

where, similarly to Eq. (35), $\delta_{\uparrow}$ and $\delta_{\downarrow}$ are, respectively, abbreviations of $\delta_0(\epsilon_F, \uparrow)$ and $\delta_0(\epsilon_F, \downarrow)$. Thus, the magnitude of the AMR, i.e., $\rho_{\parallel} - \rho_{\perp}$ in Eq. (46), is given by

$$\rho_{\parallel} - \rho_{\perp} = \frac{\hbar k_{\text{so}}^2}{\pi S n_e^2 e^2} \sin^2(\delta_{\uparrow} - \delta_{\downarrow}) \geqslant 0, \quad (49)$$

indicating that the maximal value of the AMR occurs when the difference between the phase shifts of both spin components becomes equal to $\pi/2$.

IV. SUMMARY

Using linear response theory, we have derived a formulation of the tensor of the residual electrical resistivity for the particular case of a Rashba electron gas scattering at an impurity that can be magnetic and whose magnetic moment can point in any arbitrary direction. While the obtained form is general, we applied it to the case of an Fe impurity deposited at the Au(111) surface. We performed different types of studies and investigated the nontrivial impact of the strength of spin-orbit interaction of the substrate, as well as the role of the magnetism of the impurity and of the orientation of the magnetic moment on the diagonal and off-diagonal elements of the resistivity tensor. For instance, we found that after scattering, the planar Hall effect and an anisotropic magnetoresistance occur even without incorporating the spin-orbit interaction at the impurity site if the orientation of the magnetic moment is not perpendicular to the surface. Also, an increase of the spin-orbit coupling strength induces a dramatic drop of the resistivity, which is related to a peculiar behavior of the electronic states of the Rashba electrons. Magnetism can increase the residual resistivity because of the opening of additional scattering channels, which were prohibited in the nonmagnetic case. We derive analytically and generalize the usual phenomenological functional forms of the angular dependence of the resistivity tensor elements to the cases where the magnetization points in arbitrary directions. Finally, by switching off the spin-orbit interaction, we find a simple formulation of the residual resistivity very close to the one given by Friedel for a three-dimensional electron gas [26].

Our numerical results were obtained in the s-wave approximation involving a Rashba Hamiltonian and, as discussed in the context of lifetime reduction of surface states by adatom scattering [38], it would be interesting to investigate the impact of realistic band structures computed from density functional theory on the residual resistivities and thereby assess the effect of other scattering channels besides the ones involving only surface states.

APPENDIX A: EVALUATION OF THE MOMENTUM OPERATOR MATRIX ELEMENTS

In this appendix, we will calculate the matrix elements of the momentum operator between two quantum states $i = (\varepsilon, m, \alpha)$ and $j = (\varepsilon + \hbar\omega, m', \alpha')$, in the region where the scattered wave function can be expressed by the asymptotic form given by Eq. (11), and extract only the diverging terms $\sim 1/\omega$ in the limit $\omega \to 0$. In cylindrical coordinates, the leading components of the momentum operator behave at large distances as

$$v_x \sim \frac{\hbar}{im^*}\cos\phi\,\frac{\partial}{\partial r} + \frac{\hbar}{m^*}k_{\rm so}\,\sigma_y,$$
$$v_y \sim \frac{\hbar}{im^*}\sin\phi\,\frac{\partial}{\partial r} - \frac{\hbar}{m^*}k_{\rm so}\,\sigma_x. \tag{A1}$$

With this representation of the momentum operators, we found that the diverging terms arise from the combinations

$$\langle\psi_{\varepsilon+\hbar\omega,m',\alpha'}^{\rm in,out}|m^*v_x|\psi_{\varepsilon,m,\alpha}^{\rm in,out}\rangle$$
$$\sim \frac{\hbar(\delta_{m',m+1} + \delta_{m',m-1})\delta_{\alpha\alpha'}}{2i\,\Delta k}\frac{k_{\rm M}}{k_\alpha}, \tag{A2}$$

where $\Delta k \equiv k_\alpha(\varepsilon + \hbar\omega) - k_\alpha(\varepsilon) \sim 2m^*\omega/k_{\rm M}(\varepsilon)$ is the same for both bands ($\alpha = \pm$).

By combining Eq. (11) and Eq. (A2), we obtain the momentum matrix element in the limit of $\omega \to 0$,

$$\langle\varphi_j|m^*v_x|\varphi_i\rangle \sim \frac{\hbar}{2i\,\Delta k}\frac{k_{\rm M}}{\sqrt{k_\alpha k'_\alpha}}S^x(m\alpha, m'\alpha', \varepsilon), \tag{A3}$$

where $S^x(m\alpha, m'\alpha', \varepsilon)$ is given by

$$S^x(m\alpha, m'\alpha', \varepsilon) = (\delta_{m',m+1} + \delta_{m',m-1})\delta_{\alpha\alpha'}$$
$$+ \sum_{l\alpha''} C(m\alpha, l\alpha'')C^*(m'\alpha', l+1\alpha'')$$
$$+ \sum_{l\alpha''} C(m\alpha, l\alpha'')C^*(m'\alpha', l-1\alpha''). \tag{A4}$$

Analogously, the matrix element for the y component of the momentum operator is given by

$$\langle\varphi_j|m^*v_y|\varphi_i\rangle \sim \frac{-\hbar}{2\Delta k}\frac{k_{\rm M}}{\sqrt{k_\alpha k'_\alpha}}S^y(m\alpha, m'\alpha', \varepsilon), \tag{A5}$$

with S^y defined by

$$S^y(m\alpha, m'\alpha', \varepsilon) = (\delta_{m',m+1} - \delta_{m',m-1})\delta_{\alpha\alpha'}$$
$$+ \sum_{l\alpha''} C(m\alpha, l\alpha'')C^*(m'\alpha', l+1\alpha'')$$
$$- \sum_{l\alpha''} C(m\alpha, l\alpha'')C^*(m'\alpha', l-1\alpha''). \tag{A6}$$

APPENDIX B: PHENOMENOLOGICAL DERIVATION OF THE FUNCTIONAL FORMS

Here we phenomenologically derive the functional forms, which fit the computed longitudinal and transversal components of the residual resistivity tensor. The system of interest is an adatom with a tilted magnetic moment interacting with a gas of Rashba electrons. We assume a 2D current density flowing along the x direction, J_x, which generates an electric field $\vec{E}$ [see Fig. 5(a)]. Before analyzing the general case of a tilted magnetic moment, let us recap what is expected when (i) the moment lies in plane and (ii) the moment points out of plane. In case (i), we proceed as done by Thompson *et al.* [36] and consider the x component of $\vec{E}$:

$$E_x^{(i)} = E_\parallel\cos\phi_{\vec{\rm M}} + E_\perp\sin\phi_{\vec{\rm M}}, \tag{B1}$$

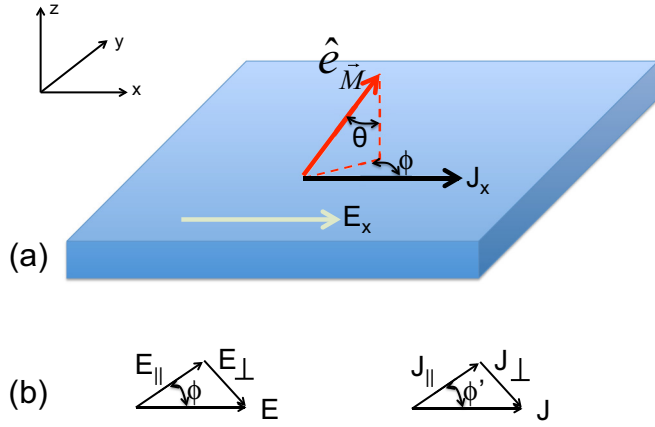FIG. 5. (a) Geometry of the system considered: a magnetic moment rotated by a polar angle θ and azimuthal angle ϕ. The current density J is related to the electric field E via the resistivity. (b) Decomposition of the electric field and the current density parallel and perpendicular to the in-plane projection of the unit vector of the magnetic moment $\hat{e}_{\vec{M}}$.

where $E_\parallel$ and $E_\perp$ are the components of the electric field parallel and perpendicular to the projection of the unit vector of the magnetic moment, $\hat{e}_{\vec{M}}$, lying in the (xy) plane (the surface plane), as depicted in Fig. 5(b). In terms of the current density and resistivity, the previous equation is then rewritten considering the parallel and perpendicular projection of the 2D current density on the direction of the magnetic moment,

$$E_x^{(i)} = J_\parallel \rho_\parallel \cos \phi_{\vec{M}} + J_\perp \rho_\perp \sin \phi_{\vec{M}}, \tag{B2}$$

as a function of the azimuthal angle $\phi_{\vec{M}}$. Also, knowing that $J = J_\parallel \cos \phi_{\vec{M}} = J_\perp \cos \phi_{\vec{M}}$ [see Fig. 5(b)] leads to

$$E_x^{(i)} = J(\rho_\parallel \cos^2 \phi_{\vec{M}} + \rho_\perp \sin^2 \phi_{\vec{M}}). \tag{B3}$$

Here, though, we give this expression in terms of the unit vector, $\hat{e}_{\vec{M}}$, defining the orientation of the moment:

$$E_x^{(i)} = J[\rho_\parallel (\hat{e}_{\vec{M}} \cdot \hat{e}_x)^2 + \rho_\perp (\hat{e}_{\vec{M}} \cdot \hat{e}_y)^2]. \tag{B4}$$

Our proposal is that in the general case of a tilted magnetic moment, the previous two equations involving $\hat{e}_{\vec{M}} \cdot \hat{e}_{x/y}$ hold. However, there is a missing contribution from the out-of-plane component of the magnetic moment. In the extreme case (ii), i.e., magnetic moment out of plane, we have

$$E_x^{(ii)} = \rho^{(ii)} J, \tag{B5}$$

and a simple generalization leads to

$$E_x^{(ii)} = \rho^{(ii)} J (\hat{e}_{\vec{M}} \cdot \hat{e}_z)^2. \tag{B6}$$

As deduced from our numerical investigation, $\rho_\parallel = \rho^{(ii)}$ [see Fig. 4(a)]. This can be explained from Fig. 3(b) for $\vec{M} \parallel z$ and Fig. 3(c) for $\vec{M} \parallel x$, where the allowed scattering processes are the same, except for the interband scattering which flips the spin but does not change the direction of $\vec{k}$. The latter affects only the spin part of the response function, not the residual resistivity (charge part) that we compute. Therefore, we get the same residual resistivity for $\vec{M} \parallel z$ and $\vec{M} \parallel x$.

Now we can add up both contributions (i) and (ii), and find

$$E_x = J[\rho_\parallel \hat{e}_{\vec{M}} \cdot (\hat{e}_x + \hat{e}_z)^2 + \rho_\perp (\hat{e}_{\vec{M}} \cdot \hat{e}_y)^2], \tag{B7}$$

which simplifies to

$$E_x = J[\rho_\parallel + (\rho_\perp - \rho_\parallel) \sin^2 \phi_{\vec{M}} \sin^2 \theta_{\vec{M}}]. \tag{B8}$$

A similar approach can be used to derive the functional forms for the transversal part of the residual resistivity tensor. Here we address the y component of $\vec{E}$ and again, after starting from the form of Thompson *et al.* [36] for case (i),

$$E_y^{(i)} = E_\parallel \sin \phi_{\vec{M}} - E_\perp \cos \phi_{\vec{M}}, \tag{B9}$$

we get

$$E_y^{(i)} = J[\rho_\parallel (\hat{e}_{\vec{M}} \cdot \hat{e}_y)^2 - \rho_\perp (\hat{e}_{\vec{M}} \cdot \hat{e}_x)^2]. \tag{B10}$$

Since there is no transversal resistivity in case (ii), the contribution $E_y^{(ii)}$ vanishes and we find

$$E_y = J(\rho_\perp - \rho_\parallel) \cos \phi_{\vec{M}} \sin \phi_{\vec{M}} \sin^2 \theta_{\vec{M}}. \tag{B11}$$

[1] E. I. Rashba, Sov. Phys. Solid State **2**, 1109 (1960).

[2] Y. A. Bychkov, E. I. Rashba: J. Phys. C: Solid State Phys. **17**, 6039 (1984).

[3] S. LaShell, B. A. McDougall, and E. Jensen, Phys. Rev. Lett. **77**, 3419 (1996).

[4] F. Reinert, G. Nicolay, S. Schmidt, D. Ehm, and S. Hüfner, Phys. Rev. B **63**, 115415 (2001).

[5] G. Nicolay, F. Reinert, S. Hüfner, and P. Blaha, Phys. Rev. B **65**, 033407 (2001).

[6] M. Hoesch, M. Muntwiler, V. N. Petrov, M. Hengsberger, L. Patthey, M. Shi, M. Falub, T. Greber, and J. Osterwalder, Phys. Rev. B **69**, 241401 (2004).

[7] A. Tamai, W. Meevasana, P. D. C. King, C. W. Nicholson, A. de la Torre, E. Rozbicki, and F. Baumberger, Phys. Rev. B **87**, 075113 (2013).

[8] G. Bihlmayer, Yu. M. Koroteev, P. M. Echenique, E. V. Chulkov, and S. Blügel, Surf. Sci. **600**, 3888 (2006).

[9] G. Bihlmayer, S. Blügel, and E. V. Chulkov, Phys. Rev. B **75**, 195414 (2007).

[10] C. R. Ast, G. Wittich, P. Wahl, R. Vogelgesang, D. Pacilé, M. C. Falub, L. Moreschini, M. Papagno, M. Grioni, and K. Kern, Phys. Rev. B **75**, 201401(R) (2007).

[11] D. Marchenko, A. Varykhalov, M. R. Scholz, G. Bihlmayer, E. I. Rashba, A. Rybkin, A. M. Shikin, and O. Rader, Nat. Commun. **3**, 1232 (2012).

[12] A. M. Shikin, A. A. Rybkina, A. S. Korshunov, Yu. B. Kudasov, N. V. Frolova, A. G. Rybkin, D. Marchenko, J. Sanchez-Barriga, A. Varykhalov, and O. Rader, New J. Phys. **15**, 095005 (2013).

[13] I. Gierz, T. Suzuki, E. Frantzeskakis, S. Pons, S. Ostanin, A. Ernst, J. Henk, M. Grioni, K. Kern, and C. R. Ast, Phys. Rev. Lett. **103**, 046803 (2009).

[14] V. M. Edelstein, Solid State Comm. **73**, 233 (1990).

[15] N. Nagaosa, J. Sinova, S. Onoda, A. H. MacDonald, and N. P. Ong, Rev. Mod. Phys. **82**, 1539 (2010).

[16] K. M. Seemann, Y. Mokrousov, A. Aziz, J. Miguel, F. Kronast, W. Kuch, M. G. Blamire, A. T. Hindmarch, B. J. Hickey, I. Souza, and C. H. Marrows, Phys. Rev. Lett. **104**, 076402 (2010).

[17] W. Thomson, Proc. R. Soc. London **8**, 546 (1857).

[18] K. L. Yau and J. T. H. Chang, J. Phys. F.: Metal Phys. **1**, 38 (1971).

[19] K. M. Seemann, F. Freimuth, H. Zhang, S. Blügel, Y. Mokrousov, D. E. Bürgler, and C. M. Schneider, Phys. Rev. Lett. **107**, 086603 (2011).

[20] M. F. Crommie, C. P. Lutz, and D. M. Eigler, Nature (London) **363**, 524 (1993).

[21] S. Lounis, A. Bringer, and S. Blügel, Phys. Rev. Lett. **108**, 207202 (2012).

[22] H. Ishida, Phys. Rev. B **52**, 10819 (1995); **54**, 10905 (1996).

[23] M. I. Trioni, H. Ishida, and G. P. Brivio, Phys. Rev. B **65**, 125413 (2002).

[24] H. A. Engel, E. I. Rashba, and B. I. Halperin, Phys. Rev. Lett. **98**, 036602 (2007).

[25] P. Sengupta and E. Bellotti, J. Phys.: Condens. Matter **27**, 405301 (2015).

[26] J. Friedel, J. Nuovo. Cim. **7**, 287 (1958).

[27] J. D. Walls, J. Huang, R. M. Westervelt, and E. J. Heller, Phys. Rev. B **73**, 035325 (2006).

[28] G. A. Fiete and E. J. Heller, Rev. Mod. Phys. **75**, 933 (2003).

[29] S. Crampin, M. H. Boon, and J. E. Inglesfield, Phys. Rev. Lett. **73**, 1015 (1994).

[30] S. Crampin and O. R. Bryant, Phys. Rev. B **54**, R17367(R) (1996).

[31] H. K. Harbury and W. Porod, Phys. Rev. B **53**, 15455 (1996).

[32] Y. Hasegawa and P. Avouris, Phys. Rev. Lett. **71**, 1071 (1993).

[33] M. F. Crommie, C. P. Lutz, and D. M. Eigler, Science **262**, 218 (1993).

[34] E. J. Heller, M. F. Crommie, C. P. Lutz, and D. M. Eigler, Nature (London) **369**, 464 (1994).

[35] N. Papanikolaou, R. Zeller, and P. H. Dederichs, J. Phys: Condens. Matter **14**, 2799 (2002).

[36] D. A. Thompson, L. T. Romankiw, and A. F. Mayadas, IEEE Trans. Magn. **11**, 1039 (1975).

[37] M. Trushin, K. Výborný, P. Moraczewski, A. A. Kovalev, J. Schliemann, and T. Jungwirth, Phys. Rev. B **80**, 134405 (2009).

[38] S. Heers, Ph. Mavropoulos, S. Lounis, R. Zeller, and S. Blügel, Phys. Rev. B **86**, 125444 (2012).